

1 **A lithium isotope perspective on the carbon and silicon cycles evolution**

2

3 Boriana Kalderon-Asael¹, Joachim A. R. Katchinoff¹, Noah J. Planavsky^{1*}, Ashleigh v.S.
4 Hood², Mathieu Dellinger³, Eric J. Bellefroid¹, David S. Jones⁴, Axel Hofmann⁵, Frantz Ossa
5 Ossa^{5,6}, Francis A. Macdonald⁷, Chunjiang Wang⁸, Terry T. Isson¹, Jack G. Murphy⁹, John A.
6 Higgins⁹, A. Joshua West¹⁰, Malcolm W. Wallace², Dan Asael¹, Philip A. E. Pogge von
7 Strandmann^{11,12*}

8

9 ¹*Yale University, Department of Geology and Geophysics, New Haven, C T 06511, USA*

10 ²*The University of Melbourne, School of Earth Sciences, Parkville, VIC, 3010, Australia*

11 ³*Durham University, Department of Geography, South Road, Durham, DH1 3LE, United*
12 *Kingdom*

13 ⁴*Amherst College Geology Department, 11 Barrett Hill Road, Amherst, Massachusetts 01002,*
14 *USA*

15 ⁵*Department of Geology, University of the Johannesburg, Johannesburg 2092, South Africa*

16 ⁶*Department of Geosciences, University of Tuebingen, 72074 Tuebingen, Germany*

17 ⁷*University of California Santa Barbara, Department of Earth Sciences, Santa Barbara, CA*
18 *93106, USA*

19 ⁸*China University of Petroleum, College of Geosciences, 18 Fuxue Road, Changping District,*
20 *Beijing 102249, China*

21 ⁹*Princeton University, Department of Geoscience, Princeton, NJ 08544, USA*

22 ¹⁰*University of Southern California, Department of Earth Sciences, 3651 Trousdale Pkwy, Los*
23 *Angeles, CA 90089, USA*

24 ¹¹*London Geochemistry and Isotope Centre (LOGIC), Institute of Earth and Planetary Sciences,*
25 *University College London and Birkbeck, University of London, Gower Street, London WC1E*
26 *6BT, UK*

27 ¹²*Institute of Geosciences, Johannes Gutenberg University, 55122 Mainz, Germany*

28

29

30 *Corresponding authors: noah.planavsky@yale.edu; p.strandmann@ucl.ac.uk;
31 boriana.kalderon-asael@yale.edu;

32

33 **The evolution of the global carbon and silicon cycles are thought to have contributed to**
34 **the long-term stability of the Earth's climate¹⁻³. Many questions remain, however,**

35 regarding the feedback mechanisms at play and more quantitative constraints on the
36 sources and sinks of these elements in the Earth's surface environments are lacking⁴⁻¹².
37 Here we argue that the lithium isotope system can be used to track processes controlling
38 the long-term carbon and silicon cycles. Based on the analysis of over 600 shallow-water
39 marine carbonate samples from 101 stratigraphic units, we construct a new carbonate
40 lithium isotope record spanning the past 3 billion years. The data suggest an increase in
41 the carbonate lithium isotope values over time, which we propose was driven by long-term
42 changes in the lithium isotopic conditions of seawater rather than changes in the
43 alterations of older samples. Based on a mass balance modelling approach, we propose
44 that the observed trend in lithium isotope values reflects a transition from the
45 Precambrian carbon and silicon cycles to those more similar to the present day. We
46 speculate that this transition may be linked to a shift to a biologically controlled marine
47 silicon cycle and the radiation of land plants^{13,14}.

48

49 Earth has maintained a clement climate for the vast majority of the past 3.5 billion years, despite
50 large changes in solar luminosity, atmospheric oxygen concentrations, and crustal evolution¹.
51 Climate stability has allowed for Earth's persistent habitation and proliferation of complex life
52 over billion-year time scales. Feedbacks within the coupled carbon (C) and silicon (Si) cycles
53 maintain this stability by regulating atmospheric carbon dioxide levels², as exemplified by the
54 continental silicate weathering feedback which removes atmospheric carbon dioxide during
55 continental weathering and transfers silicon to the ocean. This climate dependent mechanism is
56 the most commonly invoked process stabilizing Earth's long-term climate^{2,3}.

57

58 The idea that the terrestrial silicate weathering feedback played the dominant role in climate
59 regulation through Earth's history has been challenged in the last decade^{4,5}. For example, there
60 have been several recent suggestions that sedimentary and hydrothermal processes in the marine
61 realm strongly affected atmospheric carbon dioxide levels earlier in Earth's history⁶⁻⁹. It has
62 been proposed that extensive authigenic clay formation in marine sediments (reverse
63 weathering) in Si-rich oceans was a key factor leading to a warm climate through most of
64 Earth's history^{8,10}. In this view, the evolutionary radiation of siliceous organisms (sponges,
65 radiolarians, and later diatoms) forced a drop in dissolved marine Si levels and hence a marked
66 decrease in the extent of reverse weathering. There has also been extensive debate about
67 whether, how, and when land plants transformed the silicate weathering feedback^{11,12}.

68 Disagreement on fundamental aspects of the long-term C cycle demands new empirical records
69 that provide constraints on the evolution of the C and Si cycles over geological time.

70

71 The Li isotope system can be used to track processes controlling the long-term C and Si cycles.
72 Seawater Li isotope values are strongly influenced by the global extent and dominant modes of
73 clay formation and therefore can be used to determine global weathering regimes¹⁵. Lithium in
74 the crust is predominantly found in silicate minerals and the largest Li isotope fractionations
75 occur during the low-temperature formation of secondary silicate minerals—largely clays. Clay
76 minerals preferentially incorporate the lighter Li isotope (⁶Li), leaving residual waters enriched
77 in the heavier isotope (⁷Li)¹⁶. Clay formation occurs on land during incongruent silicate
78 weathering and in the oceans during off-axis seafloor alteration and during reverse weathering
79 in sediments. Therefore, clay formation in the marine and terrestrial realms has the potential to
80 drive the dissolved seawater Li isotope signature towards values heavier than the average crust
81 (crustal value is ~0‰; Ref. 17)^{15,16,18,19}. Tracking clay formation and its link to continental and
82 marine weathering processes, the Li isotope system is a powerful tool for investigating the long-
83 term controls of the C and Si cycles.

84

85 Given that carbonates can be a reliable archive of seawater $\delta^7\text{Li}$ ^{18,20,21}, we generated a new
86 carbonate Li isotope record through Earth's history. We analysed over 600 shallow-water
87 marine carbonate samples from 101 stratigraphic units that range in age from 3.0 Ga to the
88 modern (Fig. 1 and SI Tables 1 and 2). Our sampling focused on micritic carbonates but also
89 included grainstones, reef cements, microbialites, and brachiopods. Samples were selected using
90 a combination of standard and cathodoluminescence petrography (see SI for additional
91 information on sampling protocols and selected units).

92

93 A major concern with all carbonate-based proxies is whether the samples record primary signals
94 or if they have been overprinted²². The Li isotopic composition of shallow-water marine
95 carbonates in the sedimentary record depends on both the primary mineralogy of the sediment
96 (aragonite vs. calcite) and the type of alteration during early burial²³. Additionally, carbonate
97 samples can undergo late-stage alteration. Given potential uncertainties associated with these
98 processes, we tested the extent to which we can reconstruct seawater values from our carbonate
99 record in four ways (see SI). First, we generated a complementary record to our samples from
100 well-preserved early marine cements—the carbonate component that can be most robustly
101 screened for diagenetic alteration in both Phanerozoic and Precambrian rocks²⁴ (see SI Table 1;

102 Supplementary information). Second, to gauge the effects of mineralogy and diagenesis, besides
103 petrology, we analysed all samples for major/minor/trace element ratios. Third, following Ref.
104 25, we focused our sampling on carbonate units that are not from carbon isotope excursions—
105 given that these excursions are interpreted as being a signal for either short-term carbon cycle
106 perturbations or diagenetic events (see SI)^{26,27}. Lastly, a subset of our sample suite was
107 analysed for Ca isotopes, which has emerged as a powerful tracer of the extent and type of
108 diagenetic alteration in shallow-water marine carbonates^{28,29}.

109

110 Our dataset suggests a dramatic change in carbonate Li isotope values through time (Fig. 1 and
111 SI Table 2). Cainozoic and Mesozoic values range from 14.6‰ to 29.5‰ with an average of
112 $23.1 \pm 3.8\%$ 1STD ($n = 45$). This is similar to foraminifera records from the Cainozoic that range
113 from 20.1‰ to 33.7‰ with an average of $25.9 \pm 2.7\%$ 1STD ($n = 319$)^{18,30,31}. Low carbonate
114 $\delta^7\text{Li}$ values persist through most of the Palaeozoic with a mean $\delta^7\text{Li} = 10.1 \pm 4.3\%$ 1STD ($n =$
115 263) (Fig. 1). Precambrian values range from -3.8‰ to 23.5‰ but with a mean $\delta^7\text{Li} =$
116 $7.7 \pm 5.7\%$ 1STD ($n = 217$). Basic descriptive statistics suggests there are significant shifts in
117 carbonate Li isotope values through time. For instance, a Welch's ANOVA test demonstrates
118 that $\delta^7\text{Li}$ values are significantly different ($F = 273.6$, $p < 0.001$) for samples from present to
119 end-Mesozoic (0 – 252 Ma, $n = 45$), from samples spanning the Palaeozoic (252 – 541 Ma, $n =$
120 263), and samples spanning the Precambrian (541 – 3,000 Ma, $n = 217$). Critically, these low
121 values are also found in well-preserved micro-drilled marine cements (Figs. 1, 2). The general
122 trend in the $\delta^7\text{Li}$ record in carbonates resembles, to a first-order approximation, the trend in the
123 carbonate strontium isotope record through time (Fig. 1c).

124

125 Our observed trend in Li isotope values could be a signal of varying extents of alteration or a
126 signal for environmental evolution. However, several lines of evidence are inconsistent with the
127 premise that our carbonate Li isotope record reflects varying extents of alteration. Importantly,
128 the observation that low carbonate $\delta^7\text{Li}$ values, relative to modern, persist for the majority of
129 Earth's history, even after the data set is screened for detrital contamination and diagenetic
130 tracers, suggests an explanatory mechanism other than only alteration in our samples. Shallow-
131 water carbonate Li isotope values are likely to be 0‰–10‰ lighter than coeval seawater values,
132 depending on the original mineralogy and the mode of burial diagenesis (see SI; Ref. 23). Yet,
133 critically, Sr/Ca ratios and $\delta^{44/40}\text{Ca}$ analysis can be used to track the burial offset from seawater
134 in shallow-water carbonates^{23,32} (see SI), and there is no evidence for a systematic change in the
135 mode of early marine diagenesis through time that could explain the observed $\sim 15\%$ increase

136 in mean carbonate $\delta^7\text{Li}$ values (or *a priori* reason to expect such a change). Additionally, we
137 used a suite of commonly employed geochemical filters to constrain primary mineralogy
138 (Sr/Ca, Mg/Ca), track detrital contamination (Al/Ca, Rb/Ca) and diagenetic alteration (Mn/Sr,
139 Pb/Ca) (see SI for further detail). Samples screened using these methods show similar trends in
140 the unscreened Li isotope data (Fig. 1; See SI). Nonetheless, we acknowledge that some units in
141 our study may have experienced late-stage alteration that is not easily screened with typical
142 elemental tracers. Critically, however, late-stage diagenetic alteration appears to result in a shift
143 towards higher $\delta^7\text{Li}$ values³³, indicating that our carbonate record of lighter values in older
144 samples is unlikely to reflect a diagenetic bias. Building upon previous work on the effects of
145 alteration on the Li isotope system³³, we argue that if detrital contribution can be ruled out, the
146 lower boundary of the $\delta^7\text{Li}$ values will most accurately represent seawater evolution. With this
147 framework, the Li isotope record would be interpreted in a similar fashion to the scatter in the
148 long-term Sr isotope records (e.g., Ref. 34; Fig. 1d). Further, carbonate cements with
149 exceptionally well-preserved fabrics—samples that could not have undergone extensive
150 alteration after deposition (see Refs. 24,35; Fig. 1)—display the same trend as our larger bulk
151 rock dataset.

152

153 Using our carbonate record, (filtered for detrital contamination, and assuming an offset of
154 $4\pm 5\%$ from seawater; see SI; following Ref. 23), we were able to reproduce previously
155 estimated Cainozoic (Fig. S14), as well as Mesozoic and Palaeozoic $\delta^7\text{Li}_{\text{SW}}$ values (Fig. 1a).
156 Assuming this same offset for Precambrian samples, we estimate Precambrian $\delta^7\text{Li}_{\text{SW}}$ values
157 were on average 6-16‰, notably lighter than the modern oceans (31‰; Ref. 36). As with other
158 isotope systems³⁷, it will be critical to verify our reconstructed Li isotope trends in another
159 sedimentary archive. Nonetheless, we propose that the most straightforward explanation of our
160 carbonate Li isotope dataset is that there were significant changes in seawater Li isotope values
161 across Earth's history.

162

163 To evaluate the mechanisms that could be driving long-term changes in seawater Li isotope
164 values, we employed a stochastic mass balance modelling approach (Fig. 3). Specifically, we
165 use an isotope mass balance model to conduct solution space testing. This provides a means of
166 exploring possible configurations of the Li isotope system responsible for the long-term shift
167 that we observe in estimated $\delta^7\text{Li}_{\text{SW}}$ values. In our simulations, we solve Li isotope mass
168 balance at 1 Myr time intervals and allow for a wide range of possible values for high- and low-
169 temperature hydrothermal fluxes, riverine fluxes, and their isotopic values (Table SI 3). At each

170 time-step, we employ a Monte Carlo routine to re-sample the uniformly distributed key
171 parameters 1,000 times, with acceptable solutions being the ones that match our estimated,
172 error-bounded, Li isotope record (Fig. 3; see SI for the model derivation).

173

174 With our modelling approach, persistently low $\delta^7\text{Li}_{\text{SW}}$ values in the Precambrian (Fig. 3 and
175 Figs. S18-23) appear to require changes in terrestrial and marine Li cycling in Earth's past
176 relative to the modern. For instance, the only Earth system (i.e., the prominent combination of
177 Li cycle parameters) that fits our data from the Precambrian (Fig. 3) requires rivers with low Li
178 isotope values ($\delta^7\text{Li}_{\text{Riv}} < 10\text{‰}$) together with muted isotope fractionation ($\Delta^7\text{Li} < 10\text{‰}$) during
179 Li burial in the marine realm through marine authigenic clay formation (maac) and low-
180 temperature basalt alteration (lowT). Low Precambrian $\delta^7\text{Li}_{\text{SW}}$ could be related to elevated high-
181 temperature hydrothermal Li fluxes, which are a source of relatively light Li ($\sim 6.3\text{‰}$; Ref. 38).
182 However, most geophysical models show that near modern hydrothermal activity was reached
183 by the Paleoproterozoic³⁹, and some estimates suggest constant hydrothermal heat flux⁴⁰, which
184 would lead to approximately constant, long-term hydrothermal Li fluxes. Therefore, consistent
185 with our modelling results, enhanced high-temperature hydrothermal fluxes are likely not
186 responsible for the low $\delta^7\text{Li}_{\text{SW}}$ values through most of Earth's history.

187

188 The proliferation and diversification of land plants over much of the Phanerozoic has been
189 hypothesized to have fostered more extensive formation and retention of clay minerals in the
190 terrestrial realm¹³. Our work—which calls for an increase through time in $\delta^7\text{Li}_{\text{Riv}}$ values (Fig.
191 3)—supports this idea. There are multiple ways in which plants may have changed weathering,
192 but fostering soil development and increasing water-rock interaction times is one way to
193 increase the probability of clay formation¹³. There is some mineralogical evidence that also
194 supports the hypothesis that prior to the rise of land plants there was more limited pedogenic
195 clay mineral formation⁴¹. Weathering regimes may have continued to shift until the rise to
196 dominance of angiosperms at roughly 80 Ma¹⁴.

197

198 Extensive clay formation in the marine sediment column, as has been proposed for the
199 Precambrian^{8,10}, is one obvious way of changing the marine Li cycle. Our prediction of a more
200 limited effective isotope fractionation during Li burial ($\Delta^7\text{Li}_{\text{maac}}$ and $\Delta^7\text{Li}_{\text{lowT}}$) earlier in Earth's
201 history can be linked to rapid rates of clay formation, which could have led to high rates of Li
202 uptake and the reaction sites being in restricted contact with the reactant pool (seawater)⁴². For
203 the majority of Earth history, without the presence of Si-biomineralizers, seawater was highly

204 oversaturated with respect to Si phases, which could have resulted in rapid and extensive clay
205 formation⁸. This style of reverse weathering and Li removal is likely to have limited the
206 effective Li isotopic fractionation (see SI; Ref. 42). The progressive decrease in marine Si
207 concentrations over the Phanerozoic⁴³ linked to the transition to a more biologically controlled
208 Si cycle may, therefore, may have driven a shift in seawater Li isotope values.

209

210 The apparent common occurrence of low $\delta^7\text{Li}_{\text{SW}}$ values in the Precambrian and the early
211 Palaeozoic, supports the premise that the carbon cycle operated in a fundamentally different
212 mode for the majority of Earth's history compared to the present day. While we cannot use Li
213 isotope values to constrain a single Earth system, our modelling work suggests there was a
214 major shift in clay factories through Earth's history—with a likely increase in clay formation on
215 land and a decrease in clay formation in the oceans. Clay formation is a critical part of the
216 coupled C-Si cycles, suggesting that the mode of climate regulation on Earth has changed
217 dramatically through time. The shift from a Precambrian Earth state to the modern state can
218 likely be attributed to significant biological innovations—the radiation of sponges, radiolarians,
219 diatoms, and land plants. Further, our record suggests that the development of a more modern-
220 style carbon cycle tied to these ecological transitions was protracted instead of being marked by
221 step changes.

222

223 References:

- 224 1. Jaffrés, J. B. D., Shields, G. A. & Wallmann, K. The oxygen isotope evolution of
225 seawater: A critical review of a long-standing controversy and an improved geological
226 water cycle model for the past 3.4 billion years. *Earth-Science Rev.* **83**, 83–122 (2007).
- 227 2. Berner, R. A., Lasaga, A. C. & Garrels, R. M. Carbonate-silicate geochemical cycle and
228 its effect on atmospheric carbon dioxide over the past 100 million years. *Am. J. Sci.* **283**,
229 641–683 (1983).
- 230 3. West, A. J., Galy, A. & Bickle, M. Tectonic and climatic controls on silicate weathering.
231 *Earth Planet. Sci. Lett.* **235**, 211–228 (2005).
- 232 4. Isson, T. T. *et al.* Evolution of the global carbon cycle and climate regulation on Earth.
233 *Global Biogeochem. Cycles* **34**, 1–28 (2020).
- 234 5. Hilton, R. G. & West, A. J. Mountains, erosion and the carbon cycle. *Nat. Rev. Earth*
235 *Environ.* **1**, 284–299 (2020).
- 236 6. Mills, B., Lenton, T. M. & Watson, A. J. Proterozoic oxygen rise linked to shifting
237 balance between seafloor and terrestrial weathering. *Proc. Natl. Acad. Sci.* **111**, 9073–
238 9078 (2014).
- 239 7. Coogan, L. A., Gillis, K. M., Pope, M. & Spence, J. The role of low-temperature (off-
240 axis) alteration of the oceanic crust in the global Li-cycle: Insights from the Troodos
241 ophiolite. *Geochim. Cosmochim. Acta* **203**, 201–215 (2017).
- 242 8. Isson, T. T. & Planavsky, N. J. Reverse weathering as a long-term stabilizer of marine
243 pH and planetary climate. *Nature* **560**, 471–475 (2018).

- 244 9. Krissansen-Totton, J. & Catling, D. C. Constraining climate sensitivity and continental
245 versus seafloor weathering using an inverse geological carbon cycle model. *Nat.*
246 *Commun.* **8**, 1–15 (2017).
- 247 10. Krissansen-Totton, J. & Catling, D. C. A coupled carbon-silicon cycle model over Earth
248 history: Reverse weathering as a possible explanation of a warm mid-Proterozoic climate.
249 *Earth Planet. Sci. Lett.* **537**, 116181 (2020).
- 250 11. Keller, C. K. & Wood, B. D. Possibility of chemical weathering before the advent of
251 vascular land plants. *Nature* **364**, 223–225 (1993).
- 252 12. Ibarra, D. E. *et al.* Modeling the consequences of land plant evolution on silicate
253 weathering. *Am. J. Sci.* **319**, 1–43 (2019).
- 254 13. McMahon, W. J. & Davies, N. S. Evolution of alluvial mudrock forced by early land
255 plants. *Science* **359**, 1022–1024 (2018).
- 256 14. Berner, R. A. & Kothavala, Z. GEOCARB III: A revised model of atmospheric CO₂ over
257 Phanerozoic time. *Am. J. Sci.* **301**, 182–204 (2001).
- 258 15. Dellinger, M. *et al.* Riverine Li isotope fractionation in the Amazon River basin
259 controlled by the weathering regimes. *Geochim. Cosmochim. Acta* **164**, 71–93 (2015).
- 260 16. Vigier, N. *et al.* Quantifying Li isotope fractionation during smectite formation and
261 implications for the Li cycle. *Geochim. Cosmochim. Acta* **72**, 780–792 (2008).
- 262 17. Sauzéat, L., Rudnick, R. L., Chauvel, C., Garçon, M. & Tang, M. New perspectives on
263 the Li isotopic composition of the upper continental crust and its weathering signature.
264 *Earth Planet. Sci. Lett.* **428**, 181–192 (2015).
- 265 18. Misra, S. & Froelich, P. N. Lithium isotope history of cenozoic seawater: Changes in
266 silicate weathering and reverse weathering. *Science* **335**, 818–823 (2012).
- 267 19. Pogge von Strandmann, P. A. E. & Henderson, G. M. The Li isotope response to
268 mountain uplift. *Geology* **43**, 67–70 (2015).
- 269 20. Pogge von Strandmann, P. A. E. *et al.* Assessing bulk carbonates as archives for seawater
270 Li isotope ratios. *Chem. Geol.* **530**, 119338 (2019).
- 271 21. Washington, K. E. *et al.* Lithium isotope composition of modern and fossilized Cenozoic
272 brachiopods. *Geology* **48**, 27–30 (2020).
- 273 22. Fantle, M. S., Barnes, B. D. & Lau, K. V. The role of diagenesis in shaping the
274 geochemistry of the marine carbonate record. *Annu. Rev. Earth Planet. Sci.* **48**, 549–583
275 (2020).
- 276 23. Dellinger, M. *et al.* The effects of diagenesis on lithium isotope ratios of shallow marine
277 carbonates. *Am. J. Sci.* **320**, 150–184 (2020).
- 278 24. Hood, A. van S. & Wallace, M. W. Synsedimentary diagenesis in a Cryogenian reef
279 complex: Ubiquitous marine dolomite precipitation. *Sediment. Geol.* (2012)
280 doi:10.1016/j.sedgeo.2012.02.004.
- 281 25. Blättler, C. L. & Higgins, J. A. Testing Urey’s carbonate–silicate cycle using the calcium
282 isotopic composition of sedimentary carbonates. *Earth Planet. Sci. Lett.* **479**, 241–251
283 (2017).
- 284 26. Ahm, A. C. *et al.* An early diagenetic deglacial origin for basal Ediacaran “cap
285 dolostones”. *Earth Planet. Sci. Lett.* **506**, 292–307 (2019).
- 286 27. Hoffman, P. F. & Lamothe, K. G. Seawater-buffered diagenesis, destruction of carbon
287 isotope excursions, and the composition of DIC in Neoproterozoic oceans. *Proc. Natl.*
288 *Acad. Sci. U. S. A.* **116**, 18874–18879 (2019).
- 289 28. Ahm, A. S. C., Bjerrum, C. J., Blättler, C. L., Swart, P. K. & Higgins, J. A. Quantifying
290 early marine diagenesis in shallow-water carbonate sediments. *Geochim. Cosmochim.*
291 *Acta* **236**, 140–159 (2018).
- 292 29. Higgins, J. A. *et al.* Mineralogy, early marine diagenesis, and the chemistry of shallow-
293 water carbonate sediments. *Geochim. Cosmochim. Acta* **220**, 512–534 (2018).

- 294 30. Hathorne, E. C. & James, R. H. Temporal record of lithium in seawater: A tracer for
295 silicate weathering? *Earth Planet. Sci. Lett.* **246**, 393–406 (2006).
- 296 31. Hall, J. M., Chan, L. H., McDonough, W. F. & Turekian, K. K. Determination of the
297 lithium isotopic composition of planktic foraminifera and its application as a paleo-
298 seawater proxy. *Mar. Geol.* **217**, 255–265 (2005).
- 299 32. Crockford, P. W. *et al.* Reconstructing Neoproterozoic seawater chemistry from early
300 diagenetic dolomite. *Geology* **49**, 1–5 (2021).
- 301 33. Ullmann, C. V. *et al.* Partial diagenetic overprint of Late Jurassic belemnites from New
302 Zealand: Implications for the preservation potential of $\delta^7\text{Li}$ values in calcite fossils.
303 *Geochim. Cosmochim. Acta* **120**, 80–96 (2013).
- 304 34. Veizer, J. Strontium Isotopes. in *Encyclopedia of Paleoclimatology and Ancient*
305 *Environments* (ed. Gornitz, V.) 923–926 (Springler, 2009). doi:10.1007/978-1-4020-
306 4411-3_215.
- 307 35. Hood, A. van S. & Wallace, M. W. Neoproterozoic marine carbonates and their
308 paleoceanographic significance. *Glob. Planet. Change* **160**, 28–45 (2018).
- 309 36. Jeffcoate, A. B., Elliott, T., Thomas, A. & Bouman, C. Precise, small sample size
310 determinations of lithium isotopic compositions of geological reference materials and
311 modern seawater by MC-ICP-MS. *Geostand. Geoanalytical Res.* **28**, 161–172 (2004).
- 312 37. Galili, N. *et al.* The geologic history of seawater oxygen isotopes from marine iron
313 oxides. *Science* **365**, 469–473 (2019).
- 314 38. Coogan, L. A. & Dosso, S. An internally consistent, probabilistic, determination of ridge-
315 axis hydrothermal fluxes from basalt-hosted systems. *Earth Planet. Sci. Lett.* **323–324**,
316 92–101 (2012).
- 317 39. O’Neill, C., Lenardic, A., Höink, T. & Coltice, N. Mantle convection and outgassing on
318 terrestrial planets. in *Comparative climatology of terrestrial planets* (eds. Mackwell, S.
319 J., Simon-Miller, A. A., Harder, J. W. & Bullock, M. A.) 473–486 (University of Arizona
320 Press, 2013). doi:10.2458/azu_uapress_9780816530595-ch19.
- 321 40. Korenaga, J. Initiation and Evolution of Plate Tectonics on Earth: Theories and
322 Observations. *Annu. Rev. Earth Planet. Sci.* **41**, 117–151 (2013).
- 323 41. Rafiei, M. & Kennedy, M. Weathering in a world without terrestrial life recorded in the
324 Mesoproterozoic Velkerri Formation. *Nat. Commun.* **10**, (2019).
- 325 42. Clark, S. K. & Johnson, T. M. Effective isotopic fractionation factors for solute removal
326 by reactive sediments: A laboratory microcosm and slurry study. *Environ. Sci. Technol.*
327 **42**, 7850–7855 (2008).
- 328 43. Conley, D. J. *et al.* Biosilicification Drives a Decline of Dissolved Si in the Oceans
329 through Geologic Time. *Front. Mar. Sci.* **4**, (2017).
- 330 44. Pogge Von Strandmann, P. A. E. *et al.* Global climate stabilisation by chemical
331 weathering during the Hirnantian glaciation. *Geochemical Perspect. Lett.* **3**, 230–237
332 (2017).
- 333 45. Lechler, M., Pogge von Strandmann, P. A. E., Jenkyns, H. C., Prosser, G. & Parente, M.
334 Lithium-isotope evidence for enhanced silicate weathering during OAE 1a (Early Aptian
335 Selli event). *Earth Planet. Sci. Lett.* **432**, 210–222 (2015).
- 336 46. Pogge von Strandmann, P. A. E., Jenkyns, H. C. & Woodfine, R. G. Lithium isotope
337 evidence for enhanced weathering during Oceanic Anoxic Event 2. *Nat. Geosci.* **6**, 668–
338 672 (2013).
- 339 47. Shields, G. & Veizer, J. Precambrian marine carbonate isotope database: Version 1.1.
340 *Geochemistry, Geophys. Geosystems* **3**, (2002).
- 341 48. McArthur, J. M., Howarth, R. J. & Shields-Zhou, G. A. Strontium isotope stratigraphy. in
342 *A Geologic Time Scale 2012* (eds. Gradstein, F., Ogg, J., Schmitz, M. & Ogg, G.) 127–
343 144 (Cambridge University Press, 2012). doi:10.1017/CBO9780511536045.008.

- 344 49. Holland, H. D. Why the atmosphere became oxygenated: A proposal. *Geochim.*
345 *Cosmochim. Acta* **73**, 5241–5255 (2009).
- 346 50. Tajika, E. & Matsui, T. Evolution of terrestrial proto-CO₂ atmosphere coupled with
347 thermal history of the earth. *Earth Planet. Sci. Lett.* **113**, 251–266 (1992).
- 348
- 349

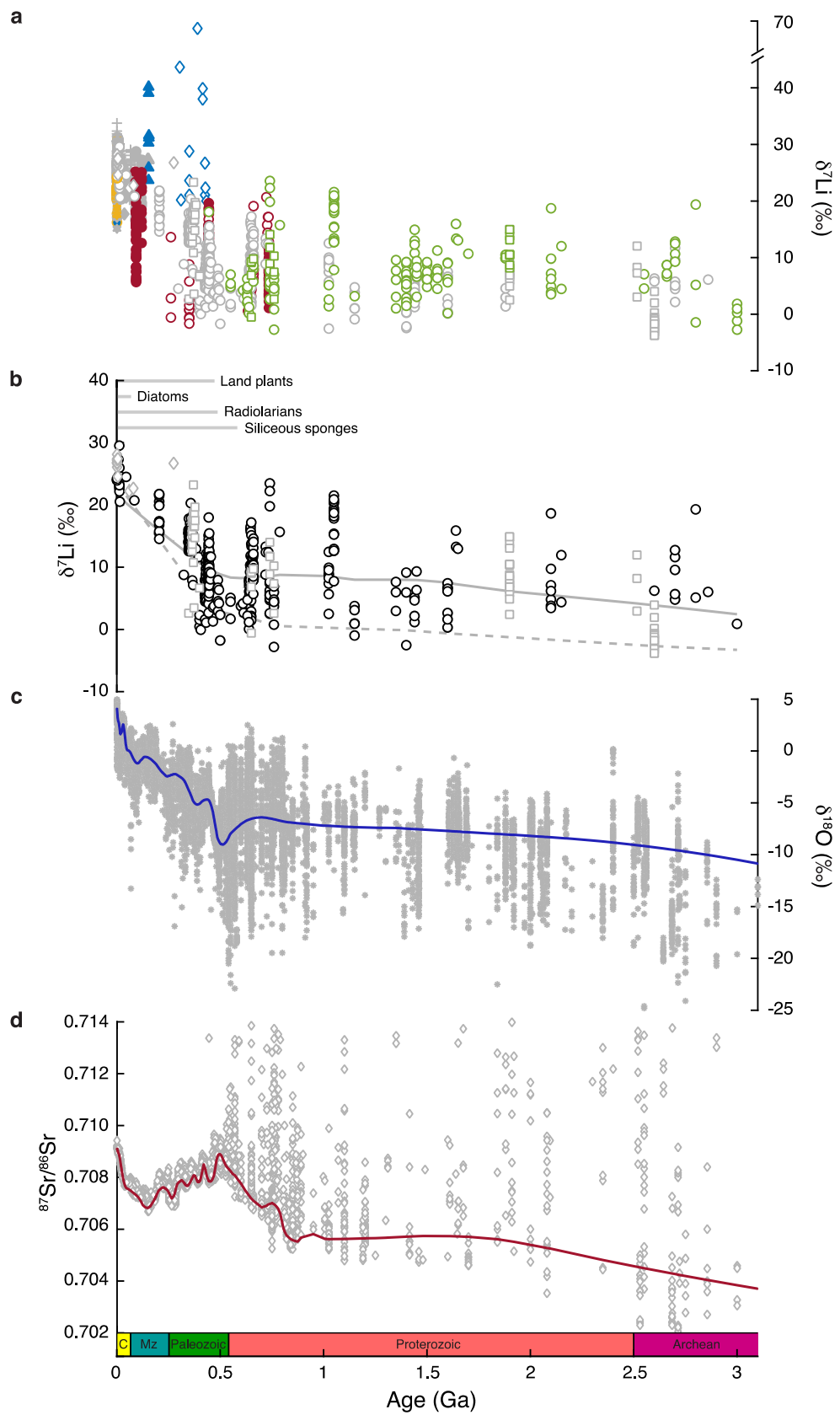
350 Acknowledgements: NJP acknowledges funding from the Alternative Earths NASA
351 Astrobiology Institute and the Packard Foundation. PPvS was funded by ERC Consolidator
352 Grant 682760 CONTROLPASTCO2. AvSH acknowledges funding from an ARC DECRA
353 (DE190100988). BKA acknowledges financial support provided by Yale Institute for
354 Biospheric Studies. We thank the Yale Peabody Museum of Natural History, Jessica Utrup and
355 Susan H. Butts for providing brachiopods and carbonate samples. We are grateful to Jeremy K.
356 Caves Rugenstein and two anonymous referees for reviews.

357

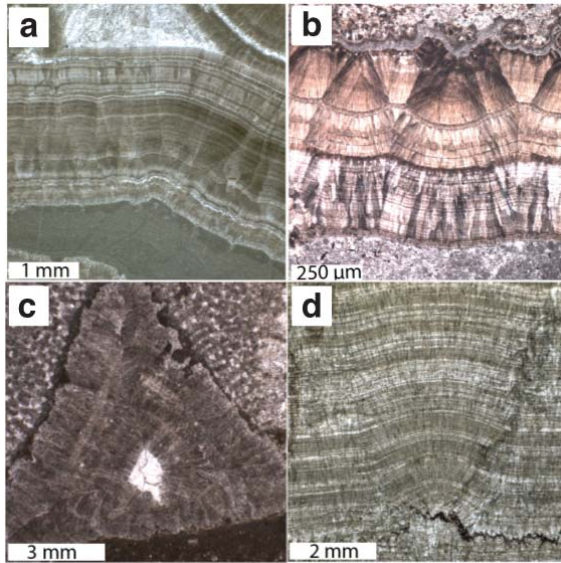
358 Author contributions: BK-A, NJP, PPvS, JARK designed the research. EJB, AvSH, DSJ, FAM,
359 MWW, JARK, AH, FOO, MD and NJP collected samples. BK-A, PPvS, JARK, MD, JGM,
360 DA, FAM conducted geochemical analyses. JARK wrote the Li isotope mass balance model.
361 BK-A wrote the Li isotope diagenetic model. BK-A, NJP, PPvS, JARK analysed the data and
362 wrote the paper. All authors contributed to the preparation of the manuscript.

363

364 Competing interests: The authors declare no competing interests.



366 **Figure 1: Isotope records in carbonates through time. a** A compilation of lithium isotope
367 values measured in different types of carbonates, including the new data from this study (open
368 symbols) and previously published data (closed symbols) ($n_{\text{total}} = 1396$; Refs.
369 18,20,21,23,30,31,33,44-46). Grey – calcite, yellow – aragonite, green – dolomite, blue -
370 diagenetically altered carbonates, and red – samples from periods of known carbon isotope
371 excursions. Shapes denote different types of carbonate archives: squares – cements, crosses –
372 foraminifera, diamonds – brachiopods, triangles – belemnites, hexagons – corals. **b** New filtered
373 lithium isotope data ($n_{\text{filtered}} = 525$; $n_{\text{new}} = 712$). Samples with indications of diagenetic alteration
374 or of high detrital input (i.e., with $\text{Al/Ca} > 0.00054$ ppm/ppm) are omitted. Light grey squares
375 denote new data from well-preserved marine cements ($n = 74$). Light grey diamonds denote
376 brachiopods. Light grey solid curve denotes a LOWESS fit of the mean of the data. Light grey
377 dashed curve denotes a LOWESS fit of the lowest ten percent of the values. **c** Oxygen isotope
378 values measured in carbonates (Ref. 47). Blue curve denotes a robust loess fit of the data. **d**
379 Strontium isotope ratios measured in carbonates (Refs. 32,48). Red curve denotes a robust loess
380 fit of the lowest ten percent of the values.



381

382

383

384

385

386

387

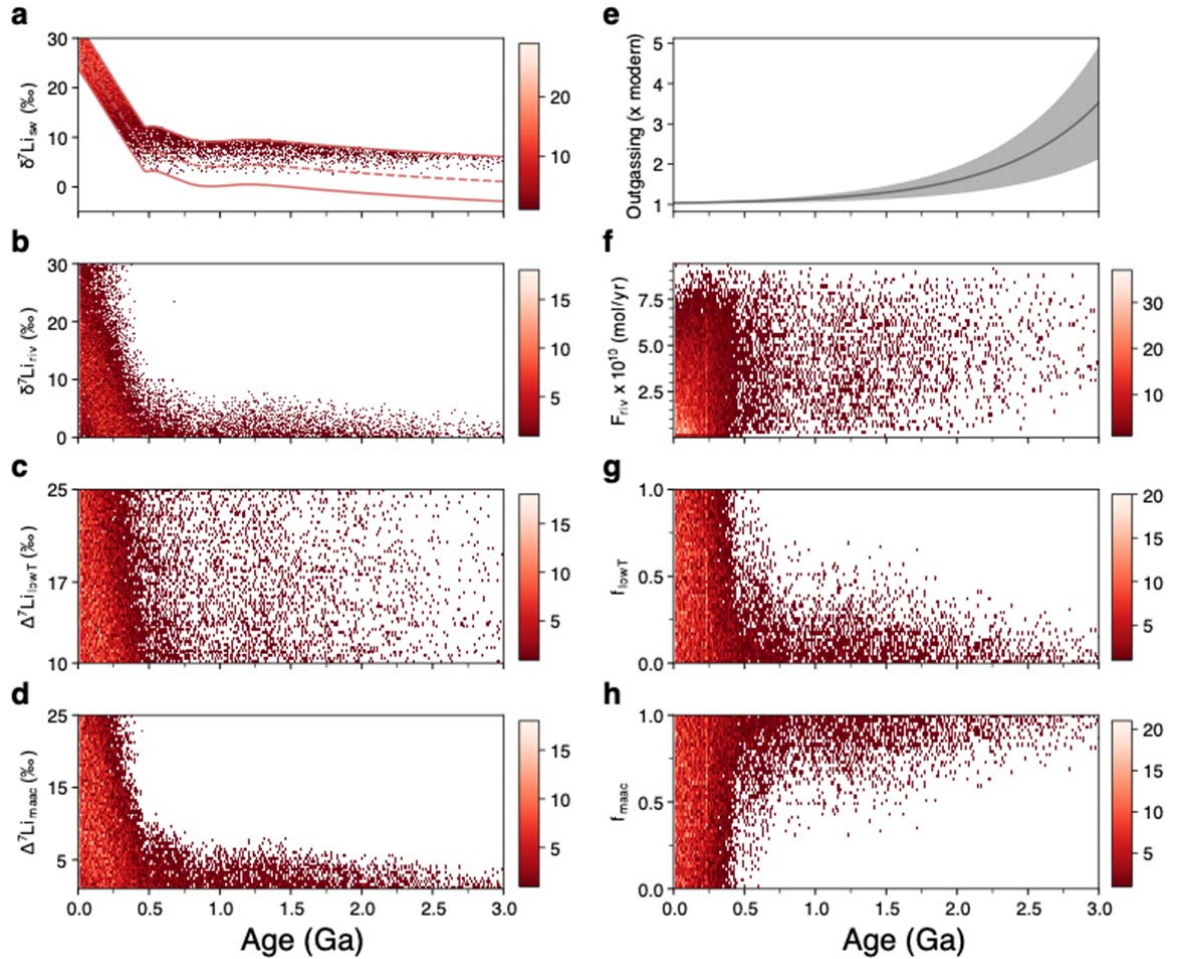
388

389

390

391

Figure 2: Thin section photomicrographs of representative well-preserved carbonates from this study. a,b Neoproterozoic carbonates: **a** Multiple generations of dolomite (and mimetically dolomitised calcite) marine cements and micrite from the Tonian Devede Fm., Namibia; **b** Well-preserved dolomitised calcite cements from the Tonian Beck Spring Dolomite, USA. **c** Paleozoic carbonate: calcite marine-cemented sponge from the Devonian Napier Formation, Australia. **d** Precambrian carbonate: calcite seafloor fans of the Neoproterozoic Campbellrand Gp., South Africa. The presence of well-preserved carbonate textures rules out extensive secondary alteration.



392
393

394 **Figure 3. Two-dimensional density heatmap of lithium isotope mass balance results.** Each
395 panel indicates the density of the parameters that successfully match our empirically
396 determined, LOWESS-smoothed Li isotope record (LOWESS conducted on lower ten percent
397 of data (dashed line in (a)), with upper and lower solid filtering bounds) through Earth's history.
398 The light red represents higher counts per bin, red represents lower counts per bin, and white
399 regions represent solution space that cannot satisfy a steady-state ($F_{in} = F_{out}$) Li seawater isotope
400 value as determined by our empirical record. Panels show **a** the Li isotope value of seawater, **b**
401 riverine Li isotope value, **c** the isotopic fractionation associated with Li removal from seawater
402 during basalt alteration ($\Delta^7\text{Li}_{lowT}$), **d** the isotopic fractionation associated with Li removal from
403 seawater during marine authigenic clay formation ($\Delta^7\text{Li}_{maac}$), **e** outgassing estimates from Refs.
404 39,49,50, **f** the riverine Li flux, **g** the proportion of Li removed through basalt alteration (f_{lowT}),
405 and **h** the proportion of Li removed through marine authigenic clay formation (f_{maac}). F_{HT} is
406 scaled linearly to a mean value of outgassing estimates. The LOWESS curve is regressed
407 through our original data with an applied calcite fractionation from seawater ($\Delta^7\text{Li} = -4\text{‰}$). The

408 lower filtering bound is -4‰ from the LOWESS curve, representing fluid buffered solutions,
409 whereas the upper bound is +5‰ from the LOWESS curve, representing the potential for any
410 samples to be aragonite.

